Hydrogen dissociation on metal surfaces

Wijzenbroek, M.

CHAPTER 2

Theory

In this chapter the theory of molecule–surface scattering is described for a diatomic molecule interacting with an ideal static surface, including methods for constructing potential energy surfaces, performing dynamics calculations on such systems as well as computing properties from the results of dynamics calculations.

2.1 Potential energy surfaces

In the treatment of the dynamics of a molecule–surface reaction, the ground state potential energy surface (PES) arises from the solution of the electronic Schrödinger equation for the problem, as is done in the framework of the Born–Oppenheimer approximation,[1] which is used throughout this thesis. The PES for a molecule interacting with a surface can be written as[2]

$$V(\vec{r},\vec{q}) = V^{6D}(\vec{r};\vec{q}_{id}) + V_{coup}(\vec{r},\vec{q}) + V_{strain}(\vec{q}), \tag{2.1}$$

where $\vec{r}$ are the molecular degrees of freedom, $\vec{q}$ the surface degrees of freedom, $V^{6D}(\vec{r};\vec{q}_{id})$ is the six-dimensional (6D) PES for the system where the surface atoms are in their ideal positions, $V_{strain}(\vec{q})$ a correction term for displacement of surface atoms in absence of the molecule and $V_{coup}(\vec{r},\vec{q})$ a further correction term for the displacement of surface atoms when the molecule is present. This "coupling" potential couples the motion of the surface atoms and the impinging molecule.

For the case of a molecule interacting with a frozen ideal surface, only $V^{6D}(\vec{r};\vec{q}_{id})$ is required. As this approximation is at the basis of most theoretical surface science studies, also in chapters 4 to 6 of this thesis, in the remainder of this section the interpolation of $V^{6D}(\vec{r};\vec{q}_{id})$ is described. The static corrugation model (SCM) is described in chapter 3.

2.1.1 Corrugation reducing procedure

For the PES of a diatomic molecule interacting with a frozen ideal surface a rather efficient interpolation procedure is available, which is called the corrugation reducing procedure (CRP).[3,4] In the CRP, the molecule–surface PES is written as

$$V^{6D}(\vec{r}) = I^{6D}(\vec{r}) + \sum_{i}^{2} V_i^{3D}(\vec{\rho}_i), \tag{2.2}$$

where $\vec{r}$ are the coordinates of the molecule, V_i^{3D} is the atom–surface potential evaluated for the coordinates $\vec{\rho}_i$ of each atom i of the molecule and I^{6D} is the so-called interpolation function, which is defined by this equation. The inclusion of V_i^{3D} serves to reduce the corrugation of the

function I^{6D} compared to V^{6D}, and I^{6D} needs to be interpolated in some way over the molecular coordinates $\vec{r}$. The atom–surface potential can further be written as

$$V_i^{3D}(\vec{\rho}_i) = I_i^{3D}(\vec{\rho}_i) + \sum_j^N V^{1D}(R_{ij}), \tag{2.3}$$

where R_{ij} is the distance between atom i of the molecule and atom j of the surface, V^{1D} a one-dimensional (1D) function which reduces the corrugation of V_i^{3D}, and I_i^{3D} another interpolation function which is defined by this equation and needs to be interpolated over the atomic coordinates $\vec{\rho}_i$. A common choice for V^{1D} is the interaction of a hydrogen atom above a top layer atom.

By performing these two steps, the corrugation of I^{6D} is reduced in the X, Y, ϑ and φ degrees of freedom with respect to V^{6D}, allowing for an easier interpolation.[3] Often in CRP potentials an interpolation scheme is used for I_i^{3D} and I^{6D} which takes into account the symmetry of the surface. An example of such a scheme, based on the method given for H_2/Cu(100) in reference 4, is described below. It is important to note that it is, in principle, possible to use other interpolation schemes than this, and that the interpolation scheme given in section 2.1.2 is clearly not the only possible scheme.

2.1.2 Symmetry-adapted interpolation

To interpolate I^{3D} and I^{6D} (or, if the CRP is not applied, V^{3D} and V^{6D}) often symmetry can be used to lower the number of points needed in the interpolation. This is because usually a periodic lattice is considered, with all the surface atoms fixed in their ideal lattice positions. Additionally, for the interpolation in the plane of the surface, additional symmetry may be present in the form of, *e.g.*, mirror planes and rotation axes. Furthermore, for the interpolation over the angular degrees of freedom even more symmetry may be present, when for example a homonuclear diatomic is considered or when the molecule is above a high-symmetry site of the surface, where an n-fold rotation axis is present. These possibilities are considered in this section and from this an interpolation scheme is derived which has been reported only for spe-

cific symmetries in the literature[3,4] and is similar to the scheme used to construct the PES for references 5 and 6.

2.1.2.1 The atom–surface potential

The atom–surface potential only depends on three degrees of freedom: the lateral coordinates u and v, and the atom–surface distance z. The z coordinate does not exhibit any symmetry due to the presence of the surface, and as such can be eliminated from the discussion of symmetry. As the u and v coordinates provide two dimensions and the PES is periodic in these degrees of freedom, the symmetry in these coordinates can be described by a wallpaper group, of which 17 exist.[7,8] For the atom–surface potential, the determination of the wallpaper group which needs to be used is simple and can be found by considering the symmetry inherent in the positions of the surface atoms. Periodic basis functions that satisfy the wallpaper group symmetry and are based on Fourier expansions have been worked out in the literature for all of the wallpaper groups.[7] In the Fourier expansion, the $\vec{r}_{\text{lat}} = (u, v)$ dependence of the PES is written as

$$V^{2D}(\vec{r}_{\text{lat}}) = \sum_{k_1,k_2} q_{k_1,k_2} \exp(i\vec{k}\vec{r}_{\text{lat}}), \tag{2.4}$$

with $\vec{k} = k_1\vec{b}_1 + k_2\vec{b}_2$, $\vec{b}_1$ and $\vec{b}_2$ the reciprocal lattice vectors, k_1 and k_2 the indices of the basis function and q_{k_1,k_2} the (complex) coefficient belonging to that basis function. Because V^{2D} represents a PES, $V^{2D} \in \mathbb{R}$, and it is therefore convenient to rewrite equation (2.4) to use real coefficients. This is done by

$$V^{2D}(\vec{r}_{\text{lat}}) = a_{0,0} + \sum_{k_1,k_2\neq(0,0)} a_{k_1,k_2} \cos(\vec{k}\vec{r}_{\text{lat}}) + b_{k_1,k_2} \sin(\vec{k}\vec{r}_{\text{lat}}). \tag{2.5}$$

Symmetry adapted basis functions $W_j(u, v)$ can then be obtained by considering for which (k_1, k_2) terms of equation (2.5) the coefficients are related by symmetry, and can contain up to twelve terms for the most symmetric wallpaper group (p6mm).[7] The first basis function is always $W_0(u, v) = 1$, and the remainder is dependent on the symmetry of the

surface. It is noted that some sine terms will cancel out due to symmetry, as $\sin(x) + \sin(-x) = 0$, and as such, these are discarded.

A simple way to satisfy the constraints on the atom–surface potential is to first obtain at N sites $V_i^{\text{atom}}(z)$, where i is a particular site. This can easily be achieved by spline interpolation over z of a number of points computed with density functional theory (DFT). When this is known, a set of N basis functions $W_j(u, v)$ needs to be chosen which are used to perform the interpolation over u and v. This yields a series of equations (one for each site at which the potential is known) of the form

$$\sum_j^N W_j(u_i, v_i) c_j(z) = V_i^{\text{atom}}(z), \tag{2.6}$$

with u_i and v_i the coordinates for site i. The above equation can be rewritten as a matrix-vector multiplication

$$\begin{pmatrix} W_1(u_1,v_1) & W_2(u_1,v_1) & \dots & W_N(u_1,v_1) \\ W_1(u_2,v_2) & W_2(u_2,v_2) & \dots & W_N(u_2,v_2) \\ \vdots & \vdots & \ddots & \vdots \\ W_1(u_N,v_N) & W_2(u_N,v_N) & \dots & W_N(u_N,v_N) \end{pmatrix} \begin{pmatrix} c_1 \\ c_2 \\ \vdots \\ c_N \end{pmatrix} = \begin{pmatrix} V_1^{\text{atom}} \\ V_2^{\text{atom}} \\ \vdots \\ V_N^{\text{atom}} \end{pmatrix} \tag{2.7}$$

or $\boldsymbol{W}\vec{c} = \vec{V}$. The coefficients can then be obtained by $\boldsymbol{W}^{-1}\vec{V} = \vec{c}$. Note that $\vec{c}$ depends on z due to $\vec{V}$, but $\boldsymbol{W}$ does not depend on z. The resulting potential can then be obtained by

$$V^{\text{3D}}(u, v, z) = \sum_j^N W_j(u, v) c_j(z). \tag{2.8}$$

The question which remains is which symmetry adapted basis functions should be used. Once the symmetry of the surface unit cell is known, and thus the symmetry of the PES is known, the basis functions can be chosen. This procedure is not entirely straightforward, and care must be taken that the matrix $\boldsymbol{W}$ remains invertible, *i.e.*, no linearly dependent rows may be present. No two basis functions should therefore give the same value for all of the geometries at which the potential is known (aliasing). One particularly important thing to note is that sometimes a lower order term needs to be discarded because the basis

function is zero at all (u, v) positions for which the potential is known. The choice of the basis set does not only depend on the symmetry of the surface, but may also depend on the sites at which the potential is known.

2.1.2.2 The molecule–surface potential

The molecule–surface potential is more difficult to interpolate as more degrees of freedom are taken into account. Not only does an interpolation need to be performed over U, V and Z, but also over r, ϑ and φ. Similar to the case for the atom–surface potential, no symmetry can be present in the Z direction, nor can there be symmetry in the internal coordinate r. The angular degrees of freedom ϑ and φ do show symmetry. Using the usual spherical coordinate system with the polar angle ϑ between 0° and 180°, and the azimuthal angle φ between 0° and 360°, $V^{6D}(\vartheta, \varphi) = V^{6D}(180° - \vartheta, \varphi + 180°)$ for homonuclear diatomic molecules like H_2. The symmetry in φ depends on whether a homonuclear diatomic is considered, but also on the presence of mirror planes and rotation axes. For a homonuclear diatomic with $\vartheta = 90°$, $V^{6D}(\vartheta = 90°, \varphi) = V^{6D}(\vartheta = 90°, \varphi + 180°)$. If the center of mass of the molecule is above a mirror plane, for some value of φ_0, $V^{6D}(\varphi - \varphi_0) = V^{6D}(\varphi_0 - \varphi)$ and V^{6D} is even around $\varphi = \varphi_0$. If the center of mass of a molecule is above a n-fold rotation axis, $V^{6D}(\varphi) = V^{6D}(\varphi + 360°/n)$.

As a first step, the interpolation over Z and r is performed for each two-dimensional (2D) cut using a 2D cubic spline interpolation. Then, at each site, the interpolation over φ is performed for each individual value of ϑ. For this interpolation the first N terms of the Fourier expansion are used, with N the number of values of φ for which the potential is known. The first few terms of this expansion, if a mirror plane passes through the point (U, V), are

$$1,\ \cos(n\varphi - \varphi_0),\ \cos(2n\varphi - \varphi_0),\ \ldots, \tag{2.9}$$

with n the order of the rotational axis present at this site and φ_0 the φ orientation at which the molecule is aligned with the mirror plane. If

no mirror plane passes through this point, the first terms are

$$1,\ \cos(n\varphi),\ \sin(n\varphi),\ \cos(2n\varphi),\ \sin(2n\varphi),\ \ldots. \tag{2.10}$$

Note that in case of a homonuclear molecule that is parallel to the surface ($\vartheta = 90°$), an additional twofold rotational symmetry is present in φ and this should be taken into account in n. The interpolation over ϑ is then performed, in which again an interpolation over the first N terms of the Fourier expansion is done. In this case, the basis is given by

$$1,\ \cos(n\vartheta),\ \sin(n\vartheta),\ \cos(2n\vartheta),\ \sin(2n\vartheta),\ \ldots, \tag{2.11}$$

with n equal to 2 for a homonuclear molecule and n equal to 1 for a heteronuclear molecule.

Finally, the interpolation over U and V needs to be performed. In the interpolation over U and V the symmetry of φ also needs to be taken into account. In a formal derivation from group theory this would result in a basis set of direct products of functions in φ and functions in U and V. This can, however, also be taken into account by mapping $V^{4D}(Z, r, \vartheta, \varphi)$ to all positions in the surface unit cell and then interpolating over U and V with a Fourier expansion similar to the one given in equation (2.5).[3,4] In this case the symmetry is imposed by applying the symmetry operators on the data rather than the basis functions. The interpolation over U and V is then based on p1 symmetry (only translation), because if the interpolation is done for a fixed φ, only for $\vartheta = 0°$ a higher symmetry than p1 is present. In order for the final PES to have the correct symmetry, all terms belonging to a particular "order" (*i.e.*, a symmetry-adapted basis function for the symmetry group of the atom–surface PES) need to be taken into account separately in the p1 interpolation. If this is not possible due to the number of points on which the potential is known, some of these terms may need to be combined.

2.2 Density functional theory

In order to obtain the potential energy for a particular geometry, which needs to be done for many geometries to compute a PES, an electronic structure method is needed. An efficient method to compute single

points for the PES is DFT.[9,10] In DFT, in contrast to other electronic structure methods, the potential energy is written as a functional of the electron density $n(\vec{r})$ of the system, instead of computing it from a wave function. As a result, the potential energy can be computed rather efficiently, as the electron density in a system with N electrons only depends on three degrees of freedom, and the method scales as N^3 instead of the N^m scaling with $m \geq 4$ for wave function based methods.

Hohenberg and Kohn[9] showed that for a system of electrons in an external potential the ground state wave function is a unique functional of $n(\vec{r})$. It was also shown that DFT is in principle variational, *i.e.*, the application of the Hamiltonian to an electron density which is not equivalent to the ground state electron density will result in a higher energy than the ground state energy.

In the DFT method proposed by Kohn and Sham,[10] a fictitious system consisting of non-interacting electrons in an effective external potential is considered. By comparing this fictitious system to the interacting system, the Schrödinger equation for the interacting system can be formulated as a set of N single-electron equations, often referred to as the Kohn–Sham equations,

$$\left[-\frac{\nabla^2}{2} + V_{\mathrm{KS}}(\vec{r})\right]\phi_i(\vec{r}) = \epsilon_i\phi_i(\vec{r}), \tag{2.12}$$

in which the first term represents the kinetic energy of the electron, and the second term the interactions between the electron and the other particles, called the Kohn–Sham potential V_{KS}. The electron density of the system can be computed by

$$n(\vec{r}) = \sum_{i=1}^{N} \left|\phi_i(\vec{r})\right|^2 \tag{2.13}$$

and the Kohn–Sham potential is given by

$$V_{\mathrm{KS}}(\vec{r}) = V_{\mathrm{ext}}(\vec{r}) + V_{\mathrm{H}}(\vec{r}) + V_{\mathrm{XC}}(\vec{r}), \tag{2.14}$$

in which $V_{\mathrm{ext}}(\vec{r})$ is the external potential, V_{H} is the Hartree (Coulomb)

potential, given by

$$V_{\mathrm{H}}(\vec{r}) = \int \frac{n(\vec{r}')}{|\vec{r} - \vec{r}'|} \mathrm{d}\vec{r}', \tag{2.15}$$

and V_{XC} the exchange–correlation (XC) potential, given by

$$V_{\mathrm{XC}}(\vec{r}) = \frac{\delta E_{\mathrm{XC}}[n]}{\delta n(\vec{r})}, \tag{2.16}$$

which represents the error made by the use of the classical Coulomb potential and the kinetic energy of the system of non-interacting electrons. The XC functional E_{XC} is not known exactly and is therefore approximated in practical calculations. These approximations are discussed in the next section.

2.2.1 The exchange–correlation functional

The unknown part of the complete density functional is called the XC functional, and it is clear that, because this part of the functional is not known exactly, the quality of practical applications of DFT depends strongly on the form of the XC functional that is chosen for a calculation. The simplest reasonable approximation is called the local density approximation (LDA), where the XC functional is written as[10]

$$E_{\mathrm{XC}}^{\mathrm{LDA}}[n] = \int n(\vec{r}) \epsilon_{\mathrm{XC}}^{\mathrm{LDA}}(n(\vec{r})) \mathrm{d}\vec{r}, \tag{2.17}$$

in which $n(\vec{r})$ is the electron density, and $\epsilon_{\mathrm{XC}}^{\mathrm{LDA}}$ is a function which depends only locally on the density. In the LDA, the assumption is therefore made that the XC energy of a system only depends locally on the electron density. For the LDA, conventionally the result from the homogeneous electron gas (HEG) is taken, which has an exact solution for the exchange energy, but needs to be approximated for the correlation energy:

$$\epsilon_{\mathrm{XC}}^{\mathrm{LDA}}(n(\vec{r})) = \epsilon_{\mathrm{X}}^{\mathrm{HEG}}(n(\vec{r})) + \epsilon_{\mathrm{C}}^{\mathrm{LDA}}(n(\vec{r})), \tag{2.18}$$

in which $\epsilon_{\mathrm{X}}^{\mathrm{HEG}}$ is given by

$$\epsilon_{\mathrm{X}}^{\mathrm{HEG}}(n(\vec{r})) = -\frac{3}{4}\left(\frac{3n(\vec{r})}{\pi}\right)^{1/3}. \tag{2.19}$$

Approximations for the HEG correlation energy are mostly based on Quantum Monte Carlo data by Ceperley and Alder.[11] Several popular approximations for the LDA correlation functional are given in references 12–14. Although LDA functionals work rather well for solids and in particular metals, a less good performance is to be expected for systems which have an electron density far away from the HEG, such as molecules.[15] The interaction of molecules with a surface is similarly not well described: for various strongly activated H_2–metal surface systems no or only a very small barrier to dissociation is found.[16–18]

The next level of approximations is the generalized gradient approximation (GGA).[19,20] In the GGA, the XC energy is still evaluated pointwise as in the LDA, but instead of the functional depending pointwise on the electron density (n) only, the gradient of the electron density (∇n) is added into the functional,

$$E_{\mathrm{XC}}^{\mathrm{GGA}}[n] = \int n(\vec{r}) \epsilon_{\mathrm{XC}}^{\mathrm{GGA}}(n(\vec{r}), \nabla n(\vec{r})) \mathrm{d}\vec{r}. \tag{2.20}$$

Such a functional is often called a semi-local functional due to the added density gradient dependence. Many semi-local functionals are written using so-called exchange or exchange–correlation enhancement factors:

$$\epsilon_{X(C)}^{\mathrm{GGA}}(n(\vec{r}), \nabla n(\vec{r})) = F_{X(C)}(n(\vec{r}), \nabla n(\vec{r})) \epsilon_{X}^{\mathrm{LDA}}(n(\vec{r})), \tag{2.21}$$

where $F_{X(C)}$ is the exchange(–correlation) enhancement factor. The exchange enhancement factor F_X is commonly written as a function of the reduced density gradient s:

$$s = \frac{\left|\nabla n(\vec{r})\right|}{2k_F(\vec{r}) n(\vec{r})} = \frac{\left|\nabla n(\vec{r})\right|}{2(3\pi^2)^{1/3} n^{4/3}(\vec{r})}. \tag{2.22}$$

Equation (2.21) provides a large amount of freedom, even if known constraints[21,22] on the XC energy are taken into account.[23,24] The number of GGA functionals that exist in the literature are therefore considerable, and libraries have been created to easily evaluate such functionals.[25] In figure 2.1 the exchange enhancement factor is shown for several popular exchange functionals.

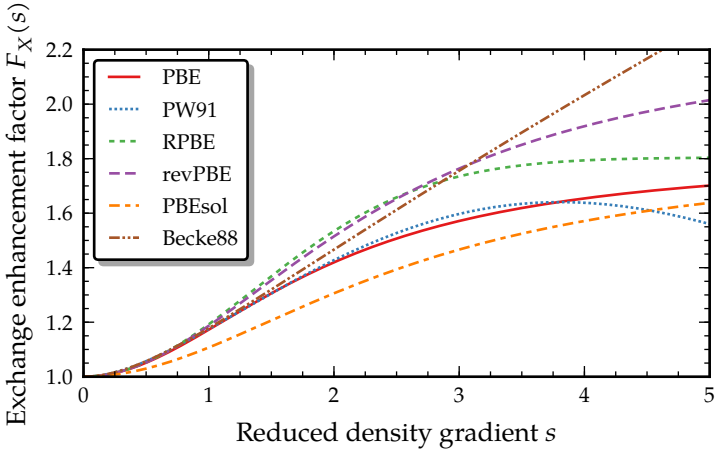

Figure 2.1 Exchange enhancement factor for several popular GGA exchange functionals.

In surface science, the PW91[21] (or the similar PBE[22]) and RPBE[23] XC functionals are rather popular. The PBE and RPBE XC functionals only differ in the exchange functional, which for PBE is determined by

$$F_X(s) = 1 + \kappa - \frac{\kappa}{1 + \mu s^2/\kappa} \tag{2.23}$$

and for RPBE by

$$F_X(s) = 1 + \kappa \left(1 - \mathrm{e}^{-\mu s^2/\kappa}\right). \tag{2.24}$$

In PBE and RPBE, the parameter κ is chosen in such a way that the Lieb–Oxford bound[26] is locally (and therefore also globally) satisfied.[22,27] μ is chosen to reproduce the LDA linear response by cancelling with correlation.[22]

For molecule–metal surface interactions, the GGA works considerably better[16–18] than the LDA, as also indicated by the wide variety of PESs computed with such methods that are described in the literature (*e.g.*, references 5, 28–32). Unfortunately, however, for solids the GGA does not always yield improvements. Only if GGA functionals specifically constructed to describe solids are used a good description of solids is obtained.[33]

Improving beyond the GGA can be done in many ways, but not all methods are feasible at present for computing a PES for a molecule interacting with a metal surface. The next step on the "Jacob's ladder" proposed by Perdew and Schmidt[34] is the meta-generalized gradient approximation (meta-GGA). In the meta-GGA, apart from the gradient of the density, also the kinetic energy density and/or the Laplacian of the density is added. One advantage for surface science is that a meta-GGA can, using the added variables, better distinguish between molecules and solids, as illustrated by the revTPSS functional.[35] It is possible to go even further, although it is not immediately apparent whether in all cases the application of such functionals to molecule–surface reactions is feasible. For example, the next step on the ladder is the "hyper-GGA", of which hybrid functionals such as B3LYP are an example.[34] In these functionals, Hartree-Fock exchange is added into the functional, which makes the computational cost for molecule–surface reactions considerable and unfeasible at present for a whole PES.

It is important to note that long range interactions such as van der Waals effects are not (properly) described when local or semi-local (*i.e.*, up to meta-GGA level) functionals are used. Various methods[36] have been used to overcome this problem, some more and some less applicable to problems involving metal surfaces. A popular method is the DFT-D3 method by Grimme *et al.*,[37] in which a pairwise potential based on C_6 coefficients computed from time-dependent density functional theory (TD-DFT) is added, in contrast to earlier methods,[38,39] where (semi)empirical values were used. Tkatchenko and Scheffler[40] have reported a method where C_6 coefficients are obtained from the mean-field ground state electron density. Other approaches are also possible. Dion *et al.*[41] have reported a "seamless" non-local XC functional (vdW-DF) that can describe van der Waals systems. Since then, other functionals have been reported[42–49] that attempt to improve over the original vdW-DF functional, by either changing the exchange functional, the correlation functional or both. The computational method of Román-Pérez and Soler[50] has allowed the vdW-DF[41] and vdW-DF2[45] correlation functionals to be evaluated self-consistently.

2.2.2 Periodic DFT using a plane wave basis set

When performing calculations of molecules on a periodic metal surface, the periodicity of the surface needs to be taken into account in order to avoid "edge" effects. One way of avoiding this is to use a sufficiently large cluster of surface atoms. Such calculations however quickly become expensive with the increased number of electrons. Another approach is to build the periodicity into the DFT calculation, by using a periodic basis set. For this basis set, plane waves are used and this method is then commonly referred to as plane wave DFT.

Although using plane waves as a basis has many upsides, there are also some downsides. First of all, generally a large number of plane waves are needed. Second, the entire simulation cell (including the adsorbate) is repeated, and not only the surface itself. This effect can be made arbitrarily small by enlarging the simulation cell so that the coverage of the surface can be decreased systematically. Finally, increasing the vacuum size in between two mirror images of a slab is penalized because more plane waves are needed. A plane wave expansion is however in other ways advantageous. For example, the basis set can be systematically improved with a single parameter and converting the wave functions between real space and momentum space can be done efficiently using fast Fourier transforms (FFTs).

2.3 Quasi-classical dynamics

In order to understand and compare to experimental measurements, dynamical properties need to be computed. In this thesis primarily the quasi-classical trajectory (QCT) method[51] is used for this purpose. In the QCT method, dynamical properties are obtained by computing trajectories for an ensemble of initial conditions. Each trajectory is propagated for a particular time until an outcome has been determined for this trajectory, such as dissociative chemisorption or scattering. When all the trajectories have been computed, reaction and scattering probabilities are obtained by counting how many trajectories show a particular outcome.

2.3.1 Initial conditions

In order to perform (quasi-)classical dynamics calculations initial positions and velocities are needed, as well as the mass of the particles. For H_2 dissociation on a metal surface the initial positions and velocities can be determined rather easily. The H_2 molecule is initially placed far away from the surface, where the potential does not depend on Z, with a particular velocity towards the surface that corresponds to the perpendicular incidence energy $E_\perp$. A random impact site is chosen and, if off-normal incidence is considered, a velocity vector is set up matching constraints from the parallel incidence energy $E_\parallel$ or the polar incidence angle ϑ_i and the azimuthal incidence angle φ_i. The orientation of the molecule ϑ and φ is randomly chosen based on the selected rotational state, with the initial angular momentum L of the molecule fixed by $L = \sqrt{J(J+1)}\hbar$ and the orientation of the angular momentum vector chosen randomly with the constraint $\cos\vartheta_L = m_J/\sqrt{J(J+1)}$, where ϑ_L is the angle between the angular momentum vector and the surface normal, and m_J is the magnetic rotational quantum number. To take into account the zero-point energy (ZPE) of the H_2 molecule, the vibrational states of the molecule are calculated using the Fourier grid Hamiltonian method.[52] The H_2 molecule is initially given the amount of energy associated with a particular vibrational state by randomly sampling positions and momenta from a 1D classical dynamics calculation of the vibrating molecule, in which the total energy is equivalent to the energy of the selected vibrational state.

2.3.2 Propagation

To integrate the equations of motion, two different propagators are used. For the *ab initio* molecular dynamics (AIMD) calculations using the VASP code,[53–56] the leapfrog algorithm implemented in VASP was used. In the leapfrog algorithm, the representation of the velocities is staggered by half a time step compared to the representation of the positions. The positions are updated by

$$\vec{x}\,(t+\Delta t) = \vec{x}\,(t) + \vec{v}\,(t+\Delta t/2)\,\Delta t, \tag{2.25}$$

and the velocities by

$$\vec{v}\,(t + \Delta t/2) = \vec{v}\,(t - \Delta t/2) + \vec{a}(t)\Delta t, \tag{2.26}$$

where the accelerations are computed from the forces F at time t. It is noted that this particular propagator is closely related to the Velocity Verlet propagator, where the velocities and positions are taken at the same time and can be evaluated by

$$\vec{v}\,(t + \Delta t/2) = \vec{v}(t) + \vec{a}(t)\Delta t/2 \tag{2.27}$$

$$\vec{x}\,(t + \Delta t) = \vec{x}(t) + \vec{v}\,(t + \Delta t/2)\,\Delta t \tag{2.28}$$

$$\vec{v}\,(t + \Delta t) = \vec{v}\,(t + \Delta t/2) + \vec{a}(t + \Delta t)\Delta t/2. \tag{2.29}$$

It is noted here that equations (2.25) and (2.28) are equivalent, while substituting equation (2.29), with the substitution $t \rightarrow t - \Delta t$, into equation (2.27) gives equation (2.26). The Velocity Verlet and leapfrog algorithms are therefore the same.[57] The advantage of the leapfrog algorithm is that with n force evaluations n time steps can be made, whereas with the Velocity Verlet algorithm the nth time step cannot be completed as equation (2.29) cannot be evaluated for the nth step without performing one extra force evaluation.

In the classical dynamics based on the CRP interpolated PESs, the extrapolation method by Stoer and Bulirsch[58] was used. In this method successively smaller time steps are used. This information is then used to extrapolate to an infinitely small time step.

2.3.3 Analysis

In a trajectory the molecule is considered to have reacted when the H–H distance r first reaches a particular value. A molecule is considered to have scattered when the molecule is far away from the surface, where no interaction is present, and also has a momentum away from the surface. After a certain amount of time t_{cut}, if neither event has occurred, the molecule is considered to be trapped.

The reaction probability P_r can then be obtained from

$$P_r = N_r/N_{\text{total}}, \tag{2.30}$$

where N_r is the number of reacted trajectories and N_{total} the total number of trajectories. Additional observables can be computed with the methods described in section 2.5. It should be noted that in quasi-classical dynamics certain observables, such as molecular beam sticking probabilities or degeneracy-averaged reaction probabilities, can also be computed by imposing specific initial conditions. In these cases P_r represents that particular observable, rather than the fully state-resolved reaction probability.

2.4 Quantum dynamics

A full description of the theory of quantum dynamics for a molecule–surface reaction is beyond the scope of this thesis. The interested reader is referred to reference 59.

For the quantum dynamics calculations a time-dependent wave packet (TDWP)[60,61] method was used. To represent the wave packet in Z, r, X and Y, a discrete variable representation (DVR)[62] was used, and to represent the wave packet in the angular degrees of freedom, a finite base representation (FBR)[63,64] was used. To transform the wave function from the FBR space to the DVR space, and *vice versa*, FFTs[65] and discrete associated Gauss–Legendre transforms[63,64] were used. To propagate the wave packet according to the time dependent Schrödinger equation, the split operator method[66] is used. The initial wave packet is placed far away from the surface, where only a negligibly small interaction is present, and is written as a product of a Gaussian wave packet for motion perpendicular to the surface, plane waves for motion parallel to the surface and a rovibrational wave function describing the initial state of the molecule.[61] The reflected wave packet is analysed using the scattering amplitude formalism[67–69] at $Z = Z_\infty$, yielding S-matrix elements for state-to-state scattering. For large r or Z, optical potentials[70] are used to absorb the reacted (r) or analysed (Z) wave packet. Scattering probabilities were obtained from S-matrix elements over the entire range of energies present in the wave packet.

The fully initial state-resolved reaction probability is defined as

$$P_r(\nu, J, m_J) = 1 - \sum_{\substack{\nu', J', m'_J, \\ n, m}} P_{\text{scat}}(\nu, J, m_J \to \nu', J', m'_J, n, m), \tag{2.31}$$

where $P_{\text{scat}}(\nu, J, m_J \to \nu', J', m'_J, n, m)$ are the state to state scattering probabilities, ν (ν'), J (J'), m_J (m'_J) the initial (final) vibrational, rotational and magnetic rotational quantum numbers, respectively, and n and m the quantum numbers for diffraction.

2.5 Computation of observables

2.5.1 Initial state-resolved reaction probability

Degeneracy averaged reaction probabilities P_{deg} can be computed by

$$P_{\text{deg}}(\nu, J) = \sum_{m_J=0}^{J} \left(2 - \delta_{m_J 0}\right) P_r(\nu, J, m_J)/(2J+1), \tag{2.32}$$

in which P_r is the fully initial state-resolved reaction probability and δ the Kronecker delta.

2.5.2 Rotational quadrupole alignment

The rotational quadrupole alignment parameter is a measure of the dependence of the reaction on the orientation of the molecule with respect to the surface. It can be written as

$$A_0^{(2)} = \left\langle 3\cos^2 \vartheta_L - 1 \right\rangle, \tag{2.33}$$

in which ϑ_L is the angle between the angular momentum vector and the surface normal. It can also be computed as[71]

$$A_0^{(2)}(\nu, J) = \frac{\sum_{m_J} P_r(\nu, J, m_J) \left(\frac{3{m_J}^2}{J(J+1)} - 1\right)}{\sum_{m_J} P_r(\nu, J, m_J)}. \tag{2.34}$$

2.5.3 Molecular beam sticking probabilities

The molecular beams used in experiments to measure sticking probabilities do generally not consist of molecules in a single state with one specific amount of energy. The experimental distributions should therefore be taken into account when comparing theoretical results to experimental data. The experimental conditions are taken into account in two steps. First, the initial state-resolved reaction probabilities are Boltzmann averaged over the rovibrational states populated in the molecular beam. Second, the experimental spread of incidence energies is taken into account. The first point is addressed by

$$R_{\text{mono}}(E_{\text{trans}}; T_{\text{n}}) = \sum_{\nu,J} F_B(\nu, J; T_{\text{n}}) P_{\text{deg}}(E_{\text{trans}}, \nu, J). \tag{2.35}$$

R_{mono} is the mono-energetic reaction probability averaged over all states present in the molecular beam obtained with a nozzle temperature T_{n}. The reaction probability of each state is weighed with the Boltzmann factor

$$F_B(\nu, J; T_{\text{n}}) = \frac{w(J) F(\nu, J; T_{\text{n}})}{\sum_{\nu', J' \equiv J \pmod 2} F(\nu', J'; T_{\text{n}})}, \tag{2.36}$$

in which

$$\begin{aligned} F(\nu, J; T_{\text{n}}) = (2J+1) \exp\left(-E_{\text{vib}}(\nu, J)/(k_B T_{\text{n}})\right) \\ \cdot \exp\left(-E_{\text{rot}}(\nu, J)/(0.8 \cdot k_B T_{\text{n}})\right). \end{aligned} \tag{2.37}$$

In equation (2.36) the summation runs only over the values of J' that have the same parity as J. E_{vib} and E_{rot} are the vibrational and rotational energy, respectively, of the (ν, J) state and k_B is the Boltzmann constant. In these equations, it is assumed that the rotational temperature of the molecules in the beam is lower than the nozzle temperature ($T_{\text{rot}} = 0.8 \cdot T_{\text{n}}$).[72] It is also assumed that the fractions of ortho- and para-H_2 and D_2 are equivalent to the high temperature limit, given by $w(J)$. This is usually the case in experiments, as the gas cylinder is stored at

room temperature and conversion of ortho- and para-hydrogen does not happen on the time scale of the experiment. For H_2, $w(J)$ is equal to $1/4$ for even J and $3/4$ for odd J. For D_2, $w(J)$ is equal to $2/3$ for even J and $1/3$ for odd J.

The mono-energetic reaction probability is then averaged over the translational energy distribution by[6]

$$R_{\text{beam}} = \frac{\int_0^\infty f(v_i; T_n) R_{\text{mono}}(E_{\text{trans}}; T_n) \mathrm{d}v_i}{\int_0^\infty f(v_i; T_n) \mathrm{d}v_i}. \tag{2.38}$$

In this equation f is the flux weighted velocity distribution, which is given by[73,74]

$$f(v_i; T_n)\mathrm{d}v_i = C{v_i}^3 \exp\left[-(v_i - v_0)^2/\alpha^2\right] \mathrm{d}v_i. \tag{2.39}$$

In equation (2.39) C is a constant, v_i the velocity of the molecule, v_0 is the stream velocity and α is a parameter describing the width of the velocity distribution.

2.5.4 Vibrational efficacy

The vibrational efficacy is a measure of how "efficiently" vibrational energy can be used to promote reaction relative to (normal) translational energy.[75,76] It can be computed by

$$\chi_\nu(J) = \frac{E_0(\nu = 0, J) - E_0(\nu = 1, J)}{E_{\text{vib}}(\nu = 1, J) - E_{\text{vib}}(\nu = 0, J)} = \frac{\Delta E_0}{\Delta E_{\text{vib}}}, \tag{2.40}$$

in which $E_{\text{vib}}(\nu, J)$ is the vibrational energy corresponding to a particular state of the gas-phase molecule and $E_0(\nu, J)$ is the energy for which $P_r(E_0; \nu, J) = P_{r,0}(\nu, J)$, where $P_{r,0}(\nu, J)$ is a particular value of the reaction probability. This reaction probability is commonly taken to be half the saturation value of the reaction probability.[75] In calculations often the convention is used that $P_{r,0}(\nu = 0, J) = P_{r,0}(\nu = 1, J)$. This convention may differ from the one often used by experimentalists if the saturation values differ for $\nu = 0$ and $\nu = 1$, or if a $P_{r,0}$ is selected that does not correspond to half the saturation value for any ν.

2.5.5 Diffraction probabilities

In chapter 4 a comparison is made between experimental and theoretical diffraction probabilities. To compare with the experimental diffraction probabilities,[77] first rovibrationally elastic diffraction probabilities were computed by

$$P_{nm}(\nu, J, m_J) = \sum_{m_J''=0}^{J} \Big(\left(2 - \delta_{m_J'' 0}\right) \cdot P_{\text{scat}}(\nu, J, m_J \to \nu' = \nu, J' = J, m_J'', n, m) \Big), \tag{2.41}$$

where P_{nm} is the rovibrationally elastic probability for scattering into the diffraction state denoted by the n and m quantum numbers. These probabilities are then degeneracy averaged by

$$P_{nm}(\nu, J) = \sum_{m_J=-J}^{J} P_{nm}(\nu, J, m_J)/(2J+1). \tag{2.42}$$

Because in experiments mostly $J = 0$ and $J = 1$ H_2 were present with a narrow energy distribution,[77,78] in particular at the lowest incidence energies, a reasonable approximation should be the use of a beam of cold n-H_2 (25 % $J = 0$, 75 % $J = 1$) with a monochromatic energy. In the calculations performed in chapter 4 this approximation is made.

References

[1] M. Born and R. Oppenheimer. Zur Quantentheorie der Molekeln. *Annalen der Physik* **389**(20), pp. 457–484, 1927.

[2] M. Bonfanti, C. Díaz, M. F. Somers, and G. J. Kroes. Hydrogen dissociation on Cu(111): the influence of lattice motion. Part I. *Physical Chemistry Chemical Physics* **13**(10), pp. 4552–4561, 2011.

[3] H. F. Busnengo, A. Salin, and W. Dong. Representation of the 6D potential energy surface for a diatomic molecule near a solid surface. *Journal of Chemical Physics* **112**(17), pp. 7641–7651, 2000.

[4] R. A. Olsen, H. F. Busnengo, A. Salin, M. F. Somers, G. J. Kroes, and E. J. Baerends. Constructing accurate potential energy surfaces for a diatomic molecule interacting with a solid surface: H_2+Pt(111) and H_2+Cu(100). *Journal of Chemical Physics* **116**(9), pp. 3841–3855, 2002.

[5] C. Díaz, E. Pijper, R. A. Olsen, H. F. Busnengo, D. J. Auerbach, and G. J. Kroes. Chemically accurate simulation of a prototypical surface reaction: H_2 dissociation on Cu(111). *Science* **326**(5954), pp. 832–834, 2009.

[6] C. Díaz, R. A. Olsen, D. J. Auerbach, and G. J. Kroes. Six-dimensional dynamics study of reactive and non reactive scattering of H_2 from Cu(111) using a chemically accurate potential energy surface. *Physical Chemistry Chemical Physics* **12**(24), pp. 6499–6519, 2010.

[7] B. Verberck. Symmetry-adapted Fourier series for the wallpaper groups. *Symmetry* **4**(3), pp. 379–426, 2012.

[8] T. J. Frankcombe, M. A. Collins, and D. H. Zhang. Modified Shepard interpolation of gas-surface potential energy surfaces with strict plane group symmetry and translational periodicity. *Journal of Chemical Physics* **137**(14), 144701, 2012.

[9] P. Hohenberg and W. Kohn. Inhomogeneous electron gas. *Physical Review* **136**(3B), B864–B871, 1964.

[10] W. Kohn and L. J. Sham. Self-consistent equations including exchange and correlation effects. *Physical Review* **140**(4A), A1133–A1138, 1965.

[11] D. M. Ceperley and B. J. Alder. Ground state of the electron gas by a stochastic method. *Physical Review Letters* **45**(7), pp. 566–569, 1980.

[12] S. H. Vosko, L. Wilk, and M. Nusair. Accurate spin-dependent electron liquid correlation energies for local spin density calculations: a critical analysis. *Canadian Journal of Physics* **58**(8), pp. 1200–1211, 1980.

[13] J. P. Perdew and Y. Wang. Accurate and simple analytic representation of the electron-gas correlation energy. *Physical Review B* **45**(23), pp. 13244–13249, 1992.

[14] J. P. Perdew and A. Zunger. Self-interaction correction to density-functional approximations for many-electron systems. *Physical Review B* **23**(10), pp. 5048–5079, 1981.

[15] S. Kurth, J. P. Perdew, and P. Blaha. Molecular and solid-state tests of density functional approximations: LSD, GGAs, and meta-GGAs. *International Journal of Quantum Chemistry* **75**(4–5), pp. 889–909, 1999.

[16] B. Hammer, K. W. Jacobsen, and J. K. Nørskov. Role of nonlocal exchange correlation in activated adsorption. *Physical Review Letters* **70**(25), pp. 3971–3974, 1993.

[17] B. Hammer, M. Scheffler, K. W. Jacobsen, and J. K. Nørskov. Multidimensional potential energy surface for H_2 dissociation over Cu(111). *Physical Review Letters* **73**(10), pp. 1400–1403, 1994.

[18] J. A. White, D. M. Bird, M. C. Payne, and I. Stich. Surface corrugation in the dissociative adsorption of H_2 on Cu(100). *Physical Review Letters* **73**(10), pp. 1404–1407, 1994.

[19] D. C. Langreth and M. J. Mehl. Beyond the local-density approximation in calculations of ground-state electronic properties. *Physical Review B* **28**(4), pp. 1809–1834, 1983.

[20] A. D. Becke. Density-functional exchange-energy approximation with correct asymptotic behavior. *Physical Review A* **38**(6), pp. 3098–3100, 1988.

[21] J. P. Perdew, J. A. Chevary, S. H. Vosko, K. A. Jackson, M. R. Pederson, D. J. Singh, and C. Fiolhais. Atoms, molecules, solids, and surfaces: applications of the generalized gradient approximation for exchange and correlation. *Physical Review B* **46**(11), pp. 6671–6687, 1992.

[22] J. P. Perdew, K. Burke, and M. Ernzerhof. Generalized gradient approximation made simple. *Physical Review Letters* **77**(18), pp. 3865–3868, 1996.

[23] B. Hammer, L. B. Hansen, and J. K. Nørskov. Improved adsorption energetics within density-functional theory using revised Perdew-Burke-Ernzerhof functionals. *Physical Review B* **59**(11), pp. 7413–7421, 1999.

[24] G. K. H. Madsen. Functional form of the generalized gradient approximation for exchange: the PBEα functional. *Physical Review B* **75**(19), 195108, 2007.

[25] M. A. L. Marques, M. J. T. Oliveira, and T. Burnus. Libxc: a library of exchange and correlation functionals for density functional theory. *Computer Physics Communications* **183**(10), pp. 2272–2281, 2012.

[26] E. H. Lieb and S. Oxford. Improved lower bound on the indirect Coulomb energy. *International Journal of Quantum Chemistry* **19**(3), pp. 427–439, 1981.

[27] A. Vela, V. Medel, and S. B. Trickey. Variable Lieb–Oxford bound satisfaction in a generalized gradient exchange-correlation functional. *Journal of Chemical Physics* **130**(24), 244103, 2009.

[28] P. Nieto, E. Pijper, D. Barredo, G. Laurent, R. A. Olsen, E. J. Baerends, G. J. Kroes, and D. Farías. Reactive and nonreactive scattering of H_2 from a metal surface is electronically adiabatic. *Science* **312**(5770), pp. 86–89, 2006.

[29] A. Gross and M. Scheffler. *Ab initio* quantum and molecular dynamics of the dissociative adsorption of hydrogen on Pd(100). *Physical Review B* **57**(4), pp. 2493–2506, 1998.

[30] J. Behler, B. Delley, S. Lorenz, K. Reuter, and M. Scheffler. Dissociation of O_2 at Al(111): the role of spin selection rules. *Physical Review Letters* **94**(3), 036104, 2005.

[31] G. A. Bocan, R. Díez Mui no, M. Alducin, H. F. Busnengo, and A. Salin. The role of exchange-correlation functionals in the potential energy surface and dynamics of N_2 dissociation on W surfaces. *Journal of Chemical Physics* **128**(15), 154704, 2008.

[32] A. Salin. Theoretical study of hydrogen dissociative adsorption on the Cu(110) surface. *Journal of Chemical Physics* **124**(10), 104704, 2006.

[33] J. P. Perdew, A. Ruzsinszky, G. I. Csonka, O. A. Vydrov, G. E. Scuseria, L. A. Constantin, X. Zhou, and K. Burke. Restoring the density-gradient expansion for exchange in solids and surfaces. *Physical Review Letters* **100**(13), 136406, 2008.

[34] J. P. Perdew and K. Schmidt. Jacob's ladder of density functional approximations for the exchange-correlation energy. *AIP Conference Proceedings* **577**(1), pp. 1–20, 2001.

[35] J. P. Perdew, A. Ruzsinszky, G. I. Csonka, L. A. Constantin, and J. Sun. Workhorse semilocal density functional for condensed matter physics and quantum chemistry. *Physical Review Letters* **103**(2), 026403, 2009.

[36] J. Klimeš and A. Michaelides. Perspective: Advances and challenges in treating van der Waals dispersion forces in density functional theory. *Journal of Chemical Physics* **137**(12), 120901, 2012.

[37] S. Grimme, J. Antony, S. Ehrlich, and H. Krieg. A consistent and accurate *ab initio* parameterization of density functional dispersion correction (DFT-D) for the 94 elements H-Pu. *Journal of Chemical Physics* **132**(15), 154104, 2010.

[38] S. Grimme. Accurate description of van der Waals complexes by density functional theory including empirical corrections. *Journal of Computational Chemistry* **25**(12), pp. 1463–1473, 2004.

[39] S. Grimme. Semiempirical GGA-type density functional constructed with a long-range dispersion correction. *Journal of Computational Chemistry* **27**(15), pp. 1787–1799, 2006.

[40] A. Tkatchenko and M. Scheffler. Accurate molecular van der Waals interactions from ground-state electron density and free-atom reference data. *Physical Review Letters* **102**(7), 073005, 2009.

[41] M. Dion, H. Rydberg, E. Schröder, D. C. Langreth, and B. I. Lundqvist. Van der Waals density functional for general geometries. *Physical Review Letters* **92**(24), 246401, 2004.

[42] V. R. Cooper. Van der Waals density functional: An appropriate exchange functional. *Physical Review B* **81**(16), 161104(R), 2010.

[43] J. Klimeš, D. R. Bowler, and A. Michaelides. Chemical accuracy for the van der Waals density functional. *Journal of Physics: Condensed Matter* **22**(2), 022201, 2010.

[44] J. Klimeš, D. R. Bowler, and A. Michaelides. Van der Waals density functionals applied to solids. *Physical Review B* **83**(19), 195131, 2011.

[45] K. Lee, E. D. Murray, L. Kong, B. I. Lundqvist, and D. C. Langreth. Higher-accuracy van der Waals density functional. *Physical Review B* **82**(8), 081101, 2010.

[46] O. A. Vydrov and T. Van Voorhis. Improving the accuracy of the nonlocal van der Waals density functional with minimal empiricism. *Journal of Chemical Physics* **130**(10), 104105, 2009.

[47] O. A. Vydrov and T. Van Voorhis. Nonlocal van der Waals density functional made simple. *Physical Review Letters* **103**(6), 063004, 2009.

[48] O. A. Vydrov and T. Van Voorhis. Implementation and assessment of a simple nonlocal van der Waals density functional. *Journal of Chemical Physics* **132**(16), 164113, 2010.

[49] O. A. Vydrov and T. Van Voorhis. Nonlocal van der Waals density functional: The simpler the better. *Journal of Chemical Physics* **133**(24), 244103, 2010.

[50] G. Román-Pérez and J. M. Soler. Efficient implementation of a van der Waals density functional: application to double-wall carbon nanotubes. *Physical Review Letters* **103**(9), 096102, 2009.

[51] M. Karplus, R. N. Porter, and R. D. Sharma. Exchange reactions with activation energy. I. Simple barrier potential for (H, H_2). *Journal of Chemical Physics* **43**(9), pp. 3259–3287, 1965.

[52] C. C. Marston and G. G. Balint-Kurti. The Fourier grid Hamiltonian method for bound state eigenvalues and eigenfunctions. *Journal of Chemical Physics* **91**(6), pp. 3571–3576, 1989.

[53] G. Kresse and J. Hafner. *Ab initio* molecular dynamics for liquid metals. *Physical Review B* **47**(1), pp. 558–561, 1993.

[54] G. Kresse and J. Furthmüller. Efficiency of *ab initio* total energy calculations for metals and semiconductors using a plane-wave basis set. *Computational Materials Science* **6**(1), pp. 15–50, 1996.

[55] G. Kresse and J. Furthmüller. Efficient iterative schemes for *ab initio* total-energy calculations using a plane-wave basis set. *Physical Review B* **54**(16), pp. 11169–11186, 1996.

[56] G. Kresse and D. Joubert. From ultrasoft pseudopotentials to the projector augmented-wave method. *Physical Review B* **59**(3), pp. 1758–1775, 1999.

[57] W. F. van Gunsteren and H. J. C. Berendsen. A leap-frog algorithm for stochastic dynamics. *Molecular Simulation* **1**(3), pp. 173–185, 1988.

[58] J. Stoer and R. Bulirsch. *Introduction to numerical analysis*. New York: Springer, 1980.

[59] G. J. Kroes and M. F. Somers. Six-dimensional dynamics of dissociative chemisorption of H_2 on metal surfaces. *Journal of Theoretical and Computational Chemistry* **04**(02), pp. 493–581, 2005.

[60] R. Kosloff. Time-dependent quantum-mechanical methods for molecular dynamics. *Journal of Physical Chemistry* **92**(8), pp. 2087–2100, 1988.

[61] E. Pijper, G. J. Kroes, R. A. Olsen, and E. J. Baerends. Reactive and diffractive scattering of H_2 from Pt(111) studied using a six-dimensional wave packet method. *Journal of Chemical Physics* **117**(12), pp. 5885–5898, 2002.

[62] J. C. Light, I. P. Hamilton, and J. V. Lill. Generalized discrete variable approximation in quantum mechanics. *Journal of Chemical Physics* **82**(3), pp. 1400–1409, 1985.

[63] G. C. Corey and D. Lemoine. Pseudospectral method for solving the time-dependent Schrödinger equation in spherical coordinates. *Journal of Chemical Physics* **97**(6), pp. 4115–4126, 1992.

[64] D. Lemoine. The finite basis representation as the primary space in multidimensional pseudospectral schemes. *Journal of Chemical Physics* **101**(12), pp. 10526–10532, 1994.

[65] D. Kosloff and R. Kosloff. A Fourier method solution for the time dependent Schrödinger equation as a tool in molecular dynamics. *Journal of Computational Physics* **52**(1), pp. 35–53, 1983.

[66] M. D. Feit, J. A. Fleck Jr., and A. Steiger. Solution of the Schrödinger equation by a spectral method. *Journal of Computational Physics* **47**(3), pp. 412–433, 1982.

[67] G. G. Balint-Kurti, R. N. Dixon, and C. C. Marston. Time-dependent quantum dynamics of molecular photofragmentation processes. *Journal of the Chemical Society, Faraday Transactions* **86**(10), pp. 1741–1749, 1990.

[68] G. G. Balint-Kurti, R. N. Dixon, and C. C. Marston. Grid methods for solving the Schrödinger equation and time dependent quantum dynamics of molecular photofragmentation and reactive scattering processes. *International Reviews in Physical Chemistry* **11**(2), pp. 317–344, 1992.

[69] R. C. Mowrey and G. J. Kroes. Application of an efficient asymptotic analysis method to molecule–surface scattering. *Journal of Chemical Physics* **103**(3), pp. 1216–1225, 1995.

[70] Á. Vibók and G. G. Balint-Kurti. Parametrization of complex absorbing potentials for time-dependent quantum dynamics. *Journal of Physical Chemistry* **96**(22), pp. 8712–8719, 1992.

[71] R. N. Zare. *Angular Momentum*. New York: Wiley, 1988.

[72] C. T. Rettner, H. A. Michelsen, and D. J. Auerbach. Quantum-state-specific dynamics of the dissociative adsorption and associative desorption of H_2 at a Cu(111) surface. *Journal of Chemical Physics* **102**(11), pp. 4625–4641, 1995.

[73] H. A. Michelsen and D. J. Auerbach. A critical examination of data on the dissociative adsorption and associative desorption of hydrogen at copper surfaces. *Journal of Chemical Physics* **94**(11), pp. 7502–7520, 1991.

[74] D. J. Auerbach. Velocity measurements by time-of-flight methods. In: *Atomic and molecular beam methods*. Ed. by G. Scoles. Vol. 1. Oxford: Oxford University Press, 1988. Chap. 14.

[75] H. A. Michelsen, C. T. Rettner, D. J. Auerbach, and R. N. Zare. Effect of rotation on the translational and vibrational energy dependence of the dissociative adsorption of D_2 on Cu(111). *Journal of Chemical Physics* **98**(10), pp. 8294–8307, 1993.

[76] C. Díaz and R. A. Olsen. A note on the vibrational efficacy in molecule–surface reactions. *Journal of Chemical Physics* **130**(9), 094706, 2009.

[77] P. Nieto, D. Farías, R. Miranda, M. Luppi, E. J. Baerends, M. F. Somers, M. J. T. C. van der Niet, R. A. Olsen, and G. J. Kroes. Diffractive and reactive scattering of H_2 from Ru(0001): experimental and theoretical study. *Physical Chemistry Chemical Physics* **13**(18), pp. 8583–8597, 2011.

[78] P. Nieto, D. Barredo, D. Farías, and R. Miranda. In-plane and out-of-plane diffraction of H_2 from Ru(001). *Journal of Physical Chemistry A* **115**(25), pp. 7283–7290, 2011.